Available online at www.sciencedirect.com
SCIENCE DIRECT
Catalysis Today 111 (2006) 248–253
CATALYSIS TODAY
www.elsevier.com/locate/cattod

Photocatalytic oxidation of CO with various oxidants by Mo oxide species highly dispersed on SiO_2 at 293 K

Takashi Kamegawa, Rumi Takeuchi, Masaya Matsuoka *, Masakazu Anpo *

Department of Applied Chemistry, Graduate School of Engineering, Osaka Prefecture University, 1-1 Gakuen-cho, Sakai, Osaka 599-8531, Japan

Received 10 May 2005; accepted 13 October 2005
Available online 20 December 2005

Abstract

The photocatalytic oxidation of CO into CO_2 with oxidants such as NO, N_2O and O_2 proceeded efficiently on a Mo/SiO_2 with high Mo dispersion under UV light irradiation. It was found that the reaction rate greatly depended on the kind and concentration of the oxidant. Photoluminescence investigations reveal the close relationship between the reaction rate and the relative concentration of the photo-excited Mo^{6+}-oxide species, i.e. charge transfer–excited–triplet state $(Mo^{5+}-O^{-})^{*}$, under steady-state reaction conditions. Moreover, the photocatalytic oxidation of CO with O_2 in excess H_2 was carried out to test suitability for applications to supplying pure H_2. This reaction was seen to proceed efficiently on Mo/SiO_2 with a high CO conversion of ~100% and CO selectivity of 99% after 180 min under UV light irradiation, showing higher photocatalytic performance than TiO_2 (P-25) photocatalyst. UV–vis, XAFS, photoluminescence and FT-IR investigations revealed that the high reactivity of the charge transfer–excited–triplet state $(Mo^{5+}-O^{-})^{*}$, with CO as well as the high reactivity of the photoreduced Mo-oxide species (Mo^{4+}-species) with O_2 to produce the original Mo-oxide species ($Mo^{6+}{=}O^{2-}$), played a crucial role in the reactions.

Keywords: Photocatalytic oxidation of CO; Mo/SiO_2 catalyst; TiO_2 (P-25); Preferential oxidation of CO in H_2; Redox cycles; Photoluminescence

1. Introduction

Recently, the catalytic oxidation of CO into CO_2 at low temperatures (200–300 K) has attracted a great deal of attention for their potential in the purification of the air as well as for the removal of CO impurity from H_2-rich gas in the development of efficient fuel cell systems [1,2]. Photocatalysis is an environmentally friendly method for CO oxidation since such a system can operate at ambient temperatures under clean and abundant solar light irradiation. It has previously been reported that transition metal oxides such as V [3–5], Cr [6,7] and Mo [8–10] highly dispersed on various oxides and the oxides incorporated within zeolite framework exhibited high photocatalytic activity for the oxidation of CO with oxidants such as O_2 and NO, under not only UV, but also visible light irradiation. However, detailed studies on the effect of the concentration and kind of oxidants on the reaction rate of photocatalytic CO oxidation reactions have still been lacking.

In the development of effective photocatalysts, photoluminescence investigations in the working state are powerful and useful techniques that can provide detailed information on the reactivity of the photo-excited active sites which play an important role in the photocatalytic reactions. A clear determination of the relationship between the concentration of the photo-excited active site and overall reaction rate under steady-state reaction conditions is crucial in elucidating the mechanisms behind photocatalytic reactions in order to improve efficiency.

In the present study, highly dispersed Mo-oxide catalysts were supported on silica by an impregnation method and characterized by in situ spectroscopic techniques such as UV–vis, XAFS, photoluminescence and FT-IR. The photocatalytic oxidation reaction of CO was performed on Mo/SiO_2 in the presence of oxidants such as O_2, NO and N_2O, with different gaseous compositions. The effect of the difference in the reactivity of the photo-excited Mo-oxide species toward the various reactant gasses on the overall photocatalytic reaction rate were investigated in detail by a photoluminescence technique. Moreover, the photocatalytic oxidation of CO to CO_2 with O_2 in excess H_2 was investigated and compared with that of TiO_2 (P-25) for the development of applicable, cheap,

* Corresponding authors.
E-mail address: anpo@chem.osakafu-u.ac.jp (M. Anpo).

0920-5861/$ – see front matter © 2005 Elsevier B.V. All rights reserved.
doi:10.1016/j.cattod.2005.10.034

non-metallic and non-polluting catalytic systems to provide pure H_2 to fuel cells.

2. Experimental

2.1. Preparation of the Mo/SiO_2 catalyst and pretreatment conditions for photocatalytic reactions and spectroscopic measurements

Mo/SiO_2 (0.6 wt% molybdenum as metal; 62.5 μmol of Mo/g-cat) was prepared by an impregnation method and, in this study, an aqueous solution of $(NH_4)_6Mo_7O_{24}{\cdot}4H_2O$ was used. After impregnation, the samples were dried at 373 K in air for 12 h and calcined at 773 K for 8 h. TiO_2 (P-25; degussa) was calcined at 723 K for 8 h in air.

Prior to the photocatalytic reactions and spectroscopic measurements, the samples were calcined in O_2 (>2.66 kPa) at 773 K (at 723 K for TiO_2) for 1 h and then degassed at 473 K for 1 h.

2.2. Apparatus and procedure

The photocatalytic reactions were carried out on the catalysts (50 or 100 mg) in a quartz cell with a flat bottom at 293 K using a high-pressure Hg lamp (Toshiba SHL-100UVQ-2) through a water filter. The reaction products were analyzed by gas chromatography.

The diffuse reflectance UV–vis spectra were recorded at room temperature with a Shimadzu UV-2200A double-beam digital spectrophotometer. The XAFS (XANES and EXAFS) spectra were obtained at the BL-19B2 facility of the SPring-8 at the Japan Synchrotron Radiation Research Institute (JASRI). The synchrotron radiation from 8.0 GeV electron storage ring was monochromatized by a Si(1 1 1) monochromator. The Mo K-edge spectra were measured in the transmission mode at room temperature. Curve fitting analysis of the EXAFS spectra was conducted on $k^3\chi(k)$ in k-space (k range = 3–12 $Å^{-1}$) with a REX2000J program (Rigaku).

The photoluminescence spectra were measured at room temperature by a SPEX Fluorolog-3 spectrofluorometer with a quartz cell directly connected to a vacuum line having stopcocks allowing gas admission or degassing.

FT-IR measurements were carried out in a specially constructed IR cell equipped with CaF_2 windows. The FT-IR spectra were recorded at room temperature with a FT-IR spectrometer (JASCO FT-IR 660 Plus) with self-supporting pellets of the samples in the transmission mode.

3. Results and discussion

3.1. Characterization of the local structures of Mo/SiO_2 catalyst

The diffuse reflectance UV–vis spectrum of Mo/SiO_2 exhibited broad absorption bands at around 220–240 and 260–280 nm (data not shown) which have been assigned to the charge transfer absorption bands of the tetrahedrally coordinated Mo^{6+}-oxide species, i.e. ($Mo^{6+}{=}O^{2-}$) species [11]. Moreover, characteristic absorption bands due to MoO_3 clusters could not be observed in the wavelength regions above 350 nm. These results indicate that a highly dispersed tetrahedral Mo^{6+}-oxide species were formed on SiO_2. In order to elucidate the local structure of this Mo^{6+}-oxide species in more detail, Mo K-edge XAFS measurements were carried out. The XANES spectrum of Mo/SiO_2 showed a characteristic preedge peak due to the 1s–4d transition of the Mo atoms, as shown in Fig. 1(A). The shape of the XANES spectrum of Mo/SiO_2 is similar to that of Na_2MoO_4 with a tetrahedral coordination (Fig. 1(B)) and the intensity of the preedge peak was higher than that of MoO_3 with an octahedral coordination (Fig. 1(C)). The Fourier transformed EXAFS (FT-EXAFS) spectrum of Mo/SiO_2 showed a peak due to the existence of neighboring oxygen atoms (Mo–O) at around 0.8–2.0 Å, while other peaks due to the presence of neighboring Mo species (Mo–O–Mo) were not observed between 3.0 and 4.0 Å. These results clearly indicate that the Mo^{6+}-oxide species mainly formed in a tetrahedrally coordinated structure on SiO_2 [12]. Moreover, curve fitting analysis of the Mo–O peak showed that the Mo^{6+}-oxides on SiO_2 had a distorted tetrahedrally coordinated structure with two shorter Mo=O double bonds and two longer Mo–O single bonds (Table 1).

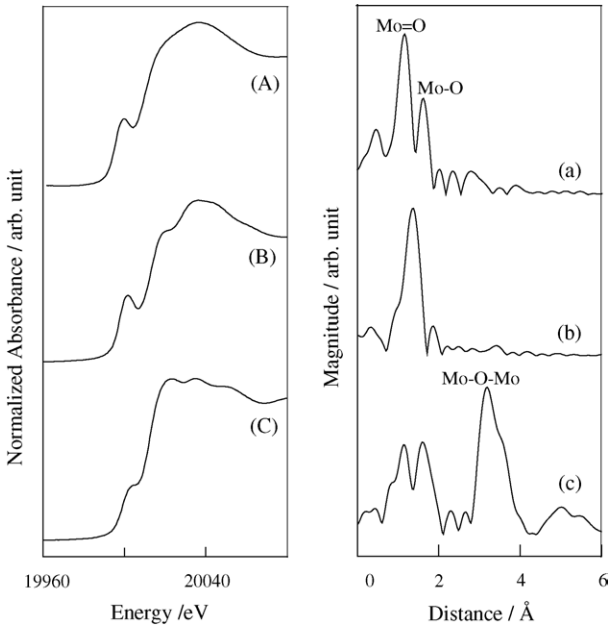

Fig. 1. XANES (A–C) and Fourier transforms of EXAFS (a–c) spectra of: (A, a), Mo/SiO_2; (B, b), Na_2MoO_4; (C, c), MoO_3.

Table 1
Results of the curve fitting analysis of the Mo K-edge EXAFS data for Mo/SiO_2 catalyst

Sample	Shell	R^a (Å)	CN[b]	σ^2 ($Å^2$)[c]
Mo/SiO_2	Mo=O	1.66	2.36	0.0016
	Mo–O	1.91	2.04	0.0017

[a] Bond distances.
[b] Coordination number.
[c] Debye–Waller factor.

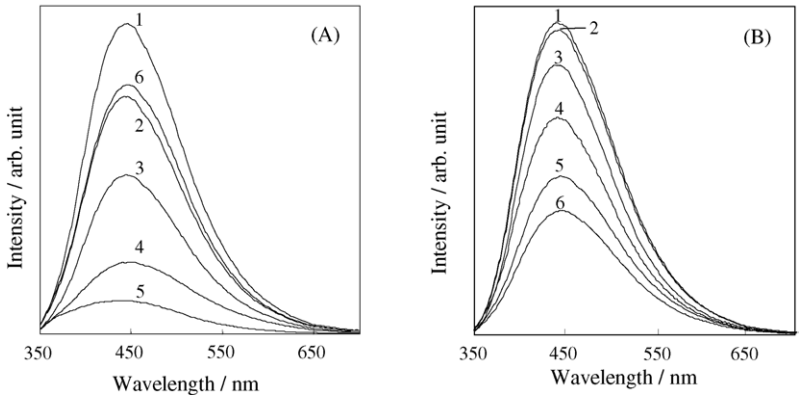

Fig. 2. Effect of the addition of CO (A) and the various quencher molecules (B) on the photoluminescence spectrum of the Mo/SiO_2 catalyst (λ_{ex} = 300 nm). A: (1) 0.0; (2) 0.0003; (3) 0.0013; (4) 0.0112; (5) 0.113 kPa; (6) degassed for 1 h after 5. B: (1) under vacuum; (2) H_2; (3) N_2O; (4) O_2; (5) CO; (6) NO. (The pressure of the quencher molecules was 0.0013 kPa and photoluminescence was measured at room temperature).

3.2. Quenching of photoluminescence by added various quencher molecules and absolute quenching rate constant of these molecules

Fig. 2 shows the effects of the addition of various quencher molecules on the photoluminescence spectrum of Mo/SiO_2 at room temperature. Under UV light irradiation at around 300 nm, Mo/SiO_2 exhibited a photoluminescence spectrum at around 400–600 nm which was attributed to the reverse radiative decay from the charge transfer–excited–triplet state of the tetrahedrally coordinated Mo-oxide species. This process is represented in the following Eq. (1) [13–15].

$$[Mo^{6+}{=}O^{2-}] \xrightarrow{h\nu} [Mo^{5+}{-}O^{-}]^{*} \xrightarrow{h\nu'} [Mo^{6+}{=}O^{2-}] \quad (1)$$

The efficient quenching of the photoluminescence by the addition of quencher molecules indicated that the $(Mo^{6+}{=}O^{2-})$ species easily interacts with these molecules in its charge transfer-excited-triplet state, $(Mo^{5+}{-}O^{-})^{*}$ state. The degassing of the quencher molecules after the quenching of the photoluminescence led to the recovery of the original photoluminescence yield except in the case of the addition of CO. For CO, the intensity of the photoluminescence was restored to 70–80% of the initial level, its extent depending on the excitation time, even after prolonged evacuation. These results clearly show that the tetrahedrally coordinated Mo^{6+}-oxide species $(Mo^{6+}{=}O^{2-})$ reacts irreversibly with CO under UV light irradiation.

The photo-physical processes on Mo/SiO_2 in the presence of the quencher molecules can be depicted as follows:

$$(Mo^{6+}{=}O^{2-}) + h\nu \xrightarrow{I} (Mo^{5+}{-}O^{-})^{*} \text{(Excitation)}$$

$$(Mo^{5+}{-}O^{-})^{*} \xrightarrow{k_{ph}} (Mo^{6+}{=}O^{2-}) + h\nu' \text{ (Photoluminescence)}$$

$$(Mo^{5+}{-}O^{-})^{*} \xrightarrow{k_{T}} (Mo^{6+}{=}O^{2-}) + h\omega \text{ (Radiationless decay)}$$

$$(Mo^{5+}{-}O^{-})^{*} + CO \xrightarrow{k_{q(CO)}} (Mo^{6+}{=}O^{2-}) + (CO)^{*}$$
(Quenching by CO)

$$(Mo^{5+}{-}O^{-})^{*} + Ox \xrightarrow{k_{q(Ox)}} (Mo^{6+}{=}O^{2-}) + (Ox)^{*}$$
(Ox=NO, N_2O andO_2) (Quenching by Ox)

where $(Mo^{6+}{=}O^{2-})$ and $(Mo^{5+}{-}O^{-})^{*}$ denote a ground state and a charge transfer–excited–triplet state, respectively and I is the intensity of the UV light, k_{ph} and k_T are the rate constants for the deactivation of $(Mo^{5+}{-}O^{-})^{*}$ by the emission of a photon ($h\nu'$) or phonon ($h\omega$), respectively and k_q ($k_{q(CO)}$ and $k_{q(Ox)}$) are the quenching rate constants by the added gasses. The Stern–Volmer Eq. (2) can be obtained for the quenching of the photoluminescence with the quencher molecules by applying steady-state treatment to the above reaction mechanism, as follows:

$$\frac{\Phi_0}{\Phi} = 1 + \tau_0 k_q [Q] \quad (2)$$

where Φ_0 and Φ show the yields of the photoluminescence in both the absence and presence of quencher molecules, respectively and τ_0, k_q ($k_{q(CO)}$ or $k_{q(Ox)}$) and $[Q]$ are the lifetimes of the charge transfer–excited–triplet state of the Mo^{6+}-oxide species ($(Mo^{5+}{-}O^{-})^{*}$) in the absence of quencher molecules, the quenching rate constant and the concentration of the quencher molecules, respectively.

Fig. 3 shows the Stern–Volmer plots for the quenching of the photoluminescence yields at room temperature resulting by the addition of various quencher molecules on Mo/SiO_2. The values of Φ_0/Φ exhibit a good linear relationship with the concentrations of the quencher molecules in low concentration regions. Moreover, the lifetime of the photoluminescence was seen to decrease with the addition of the quencher molecules. These results clearly show that the quencher molecules dynamically interact with the photo-excited Mo^{6+}-oxide species. The absolute quenching rate constants (k_q) for each gas were determined by the slope of the Stern–Volmer plots and were found to increase in the following order: $H_2 \ll N_2O \ll O_2 < CO < NO$, as shown in Fig. 3.

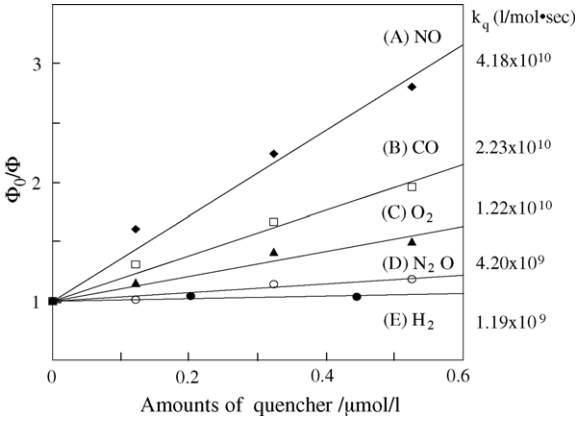

Fig. 3. Stern–Volmer plots of the Φ_0/Φ values for the yields of the photoluminescence vs. the amount of the quencher [Q] such as: (A) NO; (B) CO; (C) O_2; (D) N_2O; (E) H_2. (Lifetime of Mo/SiO_2 under vacuum: 86 μs at room temperature).

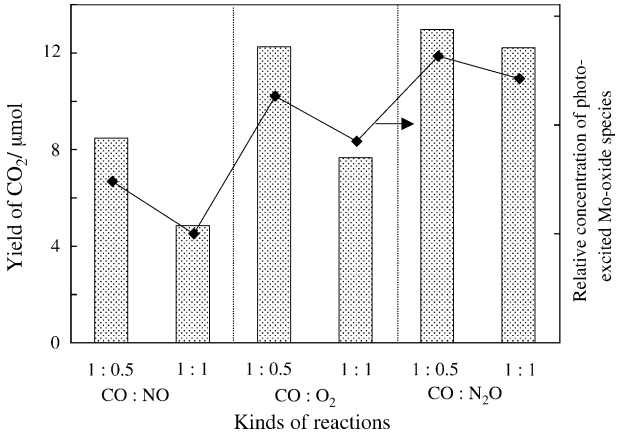

Fig. 4. Relationship between the yields of CO_2 and the relative concentrations of the charge transfer–excited–triplet state $(Mo^{5+}-O^-)^*$ species in the presence of various oxidant gasses with different concentrations. (Initial amount of gasses for CO: 28 μmol and for NO, N_2O, O_2: 28 or 14 μmol; reaction volume: 101 cm^3; amount of catalyst: 100 mg; reaction time: 0.5 h.)

3.3. Relationship between the yields of CO_2 in various photocatalytic reaction systems and relative concentrations of excited Mo-oxide species

The relationship between the concentration of the charge transfer–excited–triplet state of the Mo^{6+}-oxide species, $(Mo^{5+}-O^-)^*$ under steady-state reaction conditions and the intensity of the UV light (I) were derived from the above scheme by applying steady-state treatment, as follows:

$$[(Mo^{5+}-O^-)^*]_{vaccum} = I/(k_{ph}+k_T)\ (\tau_0 = 1/(k_{ph}+k_T))$$

$$[(Mo^{5+}-O^-)^*]_{CO,Ox} = I/(k_{ph}+k_T+k_{q(CO)}[CO] + k_{q(Ox)}[Ox])\ (Ox{=}NO, N_2O \text{ or } O_2)$$

$[(Mo^{5+}-O^-)^*]_{vacuum}$ and $[(Mo^{5+}-O^-)^*]_{CO,Ox}$ represent the concentration of the charge transfer–excited–triplet state of the Mo^{6+}-oxide species under vacuum and in the presence of quencher molecules, respectively. From these equations, the concentrations of $[(Mo^{5+}-O^-)^*]_{CO,Ox}$ can be calculated by τ_0 and k_q which were determined by photoluminescence investigations.

Fig. 4 shows the effect of the concentrations of the oxidants on the CO_2 yield in the photocatalytic oxidation of CO. When compared under the same CO concentrations, the CO_2 yield was found to be drastically affected by the kind of oxidants used. The reaction rate increased in the following order: $NO < O_2 < N_2O$, which was in opposite to the order for the quenching efficiency of these gasses, that was: $NO > O_2 > N_2O$. Moreover, the increase in the concentration of the oxidants led to the decrease in the reaction rate when compared under the same CO concentrations. These results indicate that the increase in the concentration of the oxidant gasses leads to a decrease in the reaction rate through efficient dynamic deactivation of the charge transfer–excited–triplet state, $(Mo^{5+}-O^-)^*$ species, especially in the case of an efficient quencher such as NO. In fact, as shown in Fig. 4, the reaction rate exhibited a good parallel relationship against the relative concentration of the charge transfer–excited–triplet state, $(Mo^{5+}-O^-)^*$ species, under steady-state reaction conditions ($[(Mo^{5+}-O^-)^*]^{CO,Ox}_{(relative)}$). Here, it should be noted that $[(Mo^{5+}-O^-)^*]^{CO,Ox}_{(relative)}$ can be defined by the following Eq. (3), where $[(Mo^{5+}-O^-)^*]_{CO,Ox}$ is normalized by $[(Mo^{5+}-O^-)^*]_{vacuum}$:

$$[(Mo^{5+}-O^-)^*]^{CO,Ox}_{(relative)} = \frac{[(Mo^{5+}-O^-)^*]_{CO,Ox}}{[(Mo^{5+}-O^-)^*]_{vacuum}} \quad (3)$$

These results clearly demonstrated that the charge transfer–excited–triplet state, $(Mo^{5+}-O^-)^*$ species plays a significant role in the CO oxidation reaction while the concentration of the oxidants is one of the most important factors controlling the overall reaction rate.

3.4. FT-IR measurements and redox cycles of Mo-oxide species

Fig. 5 shows the FT-IR spectra of the Mo/SiO_2 catalyst observed under UV light irradiation in the presence of CO (1.33 kPa), which led to the appearance of three peaks at 2126, 2077 and 2043 cm^{-1} due to the CO stretching vibration of the adsorbed CO species, accompanied by the formation of CO_2. The evacuation of CO in the dark led to a decrease in the intensities of the two peaks at 2126 and 2077 cm^{-1} and a simultaneous increase in the intensity of the peak at 2043 cm^{-1}. The peak at 2043 cm^{-1} completely disappeared only upon heating and degassing at temperatures above 373 K (data not shown). The peaks at 2126 and 2077 cm^{-1} and the other peak at 2043 cm^{-1} were assigned to the dicarbonyl species ($Mo^{4+}(CO)_2$) and the monocarbonyl species ($Mo^{4+}(CO)$), respectively [16]. The charge transfer–excited–triplet state, i.e. $(Mo^{5+}-O^-)^*$ species was, thus, found to react with CO accompanied by the formation of CO_2, which leads to the formation of a reduced Mo^{4+}-species and immediately other CO adsorb on it to form $Mo^{4+}(CO)_2$ and $Mo^{4+}(CO)$, as observed

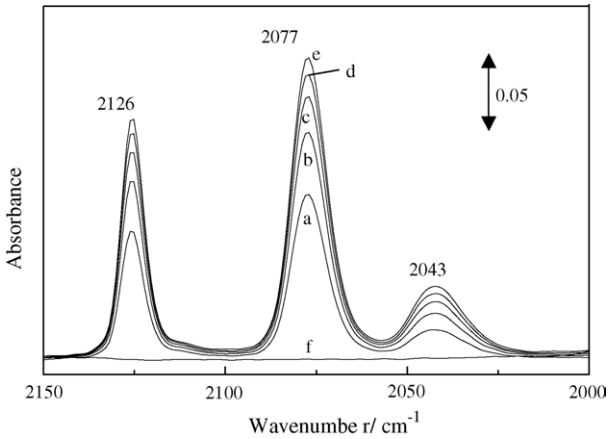

Fig. 5. (a–e) FT-IR spectra observed under UV irradiation of Mo/SiO_2 in the presence of CO (1.33 kPa) and (f) the effect of the addition of NO (1.33 kPa) in the dark on the spectrum (e). All spectra were recorded as the difference in the spectrum before and after UV light irradiation. UV light irradiation time: (a) 1; (b) 2; (c) 3; (d) 4; (e) 5 min.

by FT-IR measurements. The FT-IR peak due to the CO adsorbed species was found to disappear completely by the addition of NO accompanied by the formation of N_2O, as shown in Fig. 5(f). Moreover, the same phenomena could be observed by the addition of O_2 or N_2O (data not shown) and the formation of N_2 was observed in the case of N_2O. These results clearly indicated that the $Mo^{4+}(CO)_2$ and $Mo^{4+}(CO)$ species easily reacts with these oxidant gasses, i.e. NO, N_2O and O_2, to form the original Mo-oxide species, (Mo^{6+}=O^{2-}) species. It could, thus, be concluded that the photocatalytic oxidation of CO on Mo/SiO_2 proceeds through the following redox cycles in the presence of O_2, NO, or N_2O [8–10].

$$(Mo^{6+}{=}O^{2-}) \xrightarrow{h\nu} (Mo^{5+} - O^{-})^{*}$$

$$(Mo^{5+}{-}O^{-})^{*} + CO \rightarrow (Mo^{4+}) + CO_2$$

$$(Mo^{4+}) + \frac{1}{2}O_2 \rightarrow (Mo^{6+}{=}O^{2-})$$

$$(Mo^{4+}) + 2NO \rightarrow (Mo^{6+}{=}O^{2-}) + N_2O$$

$$(Mo^{4+}) + N_2O \rightarrow (Mo^{6+}{=}O^{2-}) + N_2$$

3.5. Photocatalytic oxidation of CO with O_2 in excess H_2

It should be noted that the quenching efficiency of H_2 for the charge transfer–excited–triplet state, $(Mo^{5+}{-}O^{-})^{*}$ was considerably low as compared to the other gasses investigated in the present study (Fig. 3). These results suggest that the reaction rate of the photocatalytic oxidation of CO was not affected by the co-existence of excess H_2.

In fact, UV light irradiation of Mo/SiO_2 in the presence of CO, O_2 and the excess H_2 led to an stoichiometric formation of CO_2 from CO and O_2, while a decrease in the amount of H_2 could hardly be observed, as shown in Fig. 6. After UV irradiation for 180 min, the concentration of CO reached below the detection limit of GC analysis (less than 8 ppm). At the

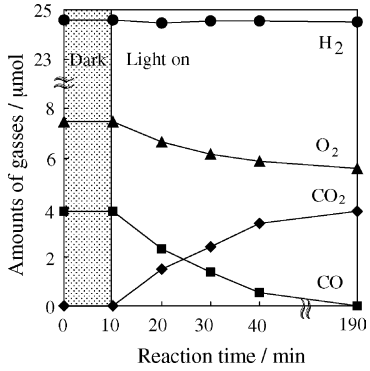

Fig. 6. Reaction time profiles of the preferential photocatalytic oxidation of CO with O_2 in the presence of H_2 on Mo/SiO_2 catalyst under UV light irradiation at 293 K. (Initial amount of gasses for CO: 3.8 μmol, O_2: 7.5 μmol and for H_2 24.6 μmol; reaction volume: 101 cm^3; amount of catalysts 50 mg).

same time, the amount of CO_2 produced as well as the amount of O_2 and H_2 consumed reached 3.8, 1.9 and 0.03 μmol, respectively. From these values, the CO conversion and selectivity were calculated to be ∼100 and 99%, respectively, by using following equation:

$$\text{CO selectivity}(\%) = \left\{ \frac{(CO_{2(t=180\,\text{min})})}{[(H_{2\ \text{initial}} - H_{2(t=180\,\text{min})}) + CO_{2\ (t=180\,\text{min})}]} \right\} \times 100$$

where $H_{2\ \text{initial}}$ refers to the initial amount of H_2 and $CO_{2(t\ =\ 180\ \text{min})}$ and $H_{2(t\ =\ 180\ \text{min})}$ are the amount of CO_2 produced and the amount of H_2 left in the gas phase after UV irradiation of 180 min, respectively.

The turnover number for the reaction defined as the ratio of the amount of CO_2 to the amount of Mo^{6+} included in the catalyst exceeded unity, indicating that the reaction proceeded photocatalytically. It should be noted that the same CO conversion rate was obtained when the reaction was conducted in the absence of H_2. Furthermore, Mo/SiO_2 catalyst exhibited high reaction rate and H_2 selectivity as compared to the TiO_2 (P-25) (CO conversion of 81% and CO selectivity of 89% after UV light irradiation of 360 min.). It has been reported that various oxygen species such as O^- (a), O_2^- (a) and O_3^- (a) derived from gaseous O_2 played an important role in the reaction [17]. The low CO selectivity observed for the reaction on TiO_2 can be ascribed to the strong and non-selective oxidation abilities of these oxygen species.

These results clearly indicated that the selective oxidation of CO with O_2 in excess H_2 proceeded with a high efficiency, showing Mo/SiO_2 to be a highly effective photocatalyst for the oxidation of CO. The reaction was shown to be closely related to the high reactivity of the charge transfer–excited–triplet state, $(Mo^{5+}{-}O^{-})^{*}$ species with CO as well as the high reactivity of the photo-formed Mo^{4+}-species with O_2 to produce the original (Mo^{6+}=O^{2-}) species, as observed by photoluminescence and FT-IR investigations. Photocatalytic systems using Mo/SiO_2 catalyst for the elimination of CO impurities from H_2-rich gas are, therefore, very promising in the development of efficient fuel cell systems with pure H_2

which can be achieved without the use of any precious noble metals such as Pt. A more detailed study of the mechanisms behind the selective photocatalytic reactions on the Mo/SiO_2 catalysts is now underway.

4. Conclusions

UV–vis, XAFS and photoluminescence investigations revealed that Mo^{6+}-oxide species exists in a highly dispersed tetrahedral coordinated structure on the Mo/SiO_2 catalyst. The photocatalytic oxidation of CO into CO_2 in the presence of oxidant gasses such as NO, N_2O and O_2 efficiently proceeded on Mo/SiO_2. Photoluminescence studies showed that the reaction rate of CO oxidation with oxidants depended proportionally on the relative concentrations of the charge transfer–excited–triplet state of the highly dispersed tetrahedral coordinated species on the Mo/SiO_2 catalyst, i.e. $(Mo^{5+}-O^{-})^{*}$ species. Moreover, photoluminescence and FT-IR investigations indicated that the $(Mo^{5+}-O^{-})^{*}$ species easily reacts with CO to form CO_2 and a reduced Mo-oxide species (Mo^{4+}-species), while the Mo^{4+}-species is easily re-oxidized to form the original Mo-oxide species ($Mo^{6+}{=}O^{2-}$) through the reaction with NO, N_2O and O_2. Thus, such unique reactivity and high redox properties were found to play a significant role in these high efficient and selective photocatalytic oxidation of CO. Also, the selective oxidation of CO with O_2 in excess H_2 proceeded photocatalytically on Mo/SiO_2 catalysts with a high CO conversion of $\sim$100% and high CO selectivity of 99%, showing higher photocatalytic performance than TiO_2 (P-25). Mo/SiO_2 catalysts are, therefore, quite promising for applications in non-noble metal catalytic systems for such significant reactions as the removal of CO from H_2-rich gas, a much desired procedure in the development of fuel cells.

References

[1] M. Okamura, S. Nakamura, S. Tsubota, M. Azuma, M. Haruta, Catal. Lett. 51 (1998) 53.
[2] Y. Minemura, S. Ito, T. Miyao, S. Naito, K. Tomishige, K. Kunimori, Chem. Commun. (2005) 102.
[3] S. Higashimoto, M. Matsuoka, S.G. Zhang, H. Yamashita, O. Kitao, H. Hidaka, M. Anpo, Microporous Mesoporous Mater. 48 (2001) 329.
[4] S. Takenaka, T. Tanaka, T. Yamazaki, T. Funabiki, S. Yoshida, J. Phys. Chem. B 101 (1997) 9035.
[5] S. Dzwigaj, M. Matsuoka, M. Anpo, M. Che, Res. Chem. Intermed. 29 (2003) 665.
[6] H. Yamashita, K. Yoshizawa, M. Ariyuki, S. Higashimoto, M. Che, M. Anpo, Chem. Commun. (2001) 435.
[7] H. Yamashita, S. Ohshiro, K. Kida, K. Yoshizawa, M. Anpo, Res. Chem. Intermed. 29 (2003) 881.
[8] R. Tsumura, S. Higashimoto, M. Matsuoka, H. Yamashita, M. Che, M. Anpo, Catal. Lett. 68 (2000) 101.
[9] A.A. Lisachenko, K.S. Chikhachev, M.N. Zakharov, L.L. Basov, B.N. Shelimov, I.R. Subbotina, M. Che, S. Coluccia, Topic Catal. 20 (2002) 119.
[10] I.R. Subbotina, B.N. Shelimov, V.B. Kazansky, A.A. Lisachenko, M. Che, S. Coluccia, J. Catal. 184 (1999) 390.
[11] N. Giordano, J.C.J. Bart, A. Vaghi, A. Castellan, G. Martinotti, J. Catal. 36 (1975) 81.
[12] R. Radhakrishnan, C. Reed, S.T. Oyama, M. Seman, J.N. Kondo, K. Domen, Y. Ohminami, K. Asakura, J. Phys. Chem. B 105 (2001) 8519.
[13] M. Anpo, M. Che, Adv. Catal. 44 (1999) 119.
[14] M. Anpo, M. Kondo, S. Coluccia, C. Louis, M. Che, J. Am. Chem. Soc. 111 (1989) 8791.
[15] M. Anpo, M. Kondo, Y. Kubokawa, C. Louis, M. Che, J. Chem. Soc. Faraday Trans. 1 (84) (1988) 2771.
[16] C.C. Williams, J.G. Ekerdt, J. Phys. Chem. 97 (1993) 6843.
[17] S. Sato, T. Kadowaki, J. Catal. 106 (1987) 295.